Supramolecular Chemistry
Publication details, including instructions for authors and subscription information:
http://www.informaworld.com/smpp/title~content=t713649759

Fluorophore-labeled Polyamidoamine (PAMAM) Dendritic Architectures: Synthesis and Fluorescence Sensing Properties

Samaresh Ghosh[a]; Ajit K. Banthia[a]
[a] Materials Science Centre, Indian Institute of Technology, Kharagpur, India

To cite this Article Ghosh, Samaresh and Banthia, Ajit K.(2004) 'Fluorophore-labeled Polyamidoamine (PAMAM) Dendritic Architectures: Synthesis and Fluorescence Sensing Properties', Supramolecular Chemistry, 16: 7, 487 — 494
To link to this Article: DOI: 10.1080/10610270410001721953
URL: http://dx.doi.org/10.1080/10610270410001721953

Supramolecular Chemistry, October–November 2004, Vol. 16 (7), pp. 487–494

Fluorophore-labeled Polyamidoamine (PAMAM) Dendritic Architectures: Synthesis and Fluorescence Sensing Properties

SAMARESH GHOSH and AJIT K. BANTHIA*

Materials Science Centre, Indian Institute of Technology, Kharagpur 721302, India

Received (in Southampton, UK) 28 January 2004; Accepted 7 May 2004

Novel polyamidoamine (PAMAM) dendrimers ($G = 0.5–2.5$) with a naphthalene core unit have been prepared. They were found to display acid as well as metal ion sensitive fluorescence signal amplification, making them of potential use as chemosensing materials. PAMAM dendritic wedges as well as naphthalene-centered PAMAM dendrimers were characterized by FT-IR, ^{1}H and ^{13}C NMR spectroscopic methods and elemental analysis.

Keywords: Polyamidoamine; Dendrimer; Fluorescence; Naphthalene

INTRODUCTION

Fluorescent chemosensors are of considerable importance in both chemistry and biology [1,2]. Naphthalene units are interesting and potentially useful luminescent chromophore units that have been used in the development of novel macromolecular fluorescent chemosensors. In this context, labeling of dendritic macromolecular architectures with fluorophore units is one of the viable routes of generating suitable luminescent dendritic macromolecules [3–9] having well-defined branched and compartmentalized structures. Considerable interest in polyamidoamine (PAMAM) dendritic macromolecules [10–16] has arisen because of their novel structural properties and wide range of potential applications. Constructing a PAMAM dendrimer around a luminescent group could profitably alter the luminescence signals in the macromolecular structure and amplify the signals for sensing purposes. Our preliminary investigations into the synthesis of a luminescent naphthalene-centered PAMAM dendrimer [7] was published previously. In this paper, we report a full account of the divergent construction of naphthalene-centered novel PAMAM dendrimers ($G = 0.5–2.5$) together with their fluorescence signaling in response to other molecules (e.g. carboxylic acids, metal ions, etc).

RESULTS AND DISCUSSION

Synthesis of Naphthalene-centered PAMAM Dendrimers

The routes to the synthesis of ester-terminated PAMAM dendritic wedges **1**–**3** as shown in Scheme 1 follow those previously reported [7,13] by us for the synthesis of azobenzene- and naphthalene-based PAMAM dendrimers.

The synthesized dendritic wedges having one hydroxyl group at the focal point thus offer a myriad of possibilities of designing unique structures with specific properties through coupling them in various polyfunctional core molecules. The syntheses of titled dendrimers **4**–**6** were carried out by using 1,5-dihydroxynaphthalene, an aliphatic dicarboxylic acid chloride (e.g. sebacoyl chloride) and ester-terminated dendritic wedges **1**–**3** according to Scheme 2. The dendrimers, isolated in 50–55% yield, were gummy in nature and soluble in halogenated organic solvents like $CHCl_3$, CH_2Cl_2.

The dendritic wedges and the dendrimers were characterized by means of spectroscopic techniques and elemental analysis. FT-IR spectra of PAMAM

*Corresponding author. Fax: +91-3222-255303. E-mail: ajitbanthia2000@yahoo.co.in

ISSN 1061-0278 print/ISSN 1029-0478 online © 2004 Taylor & Francis Ltd
DOI: 10.1080/10610270410001721953

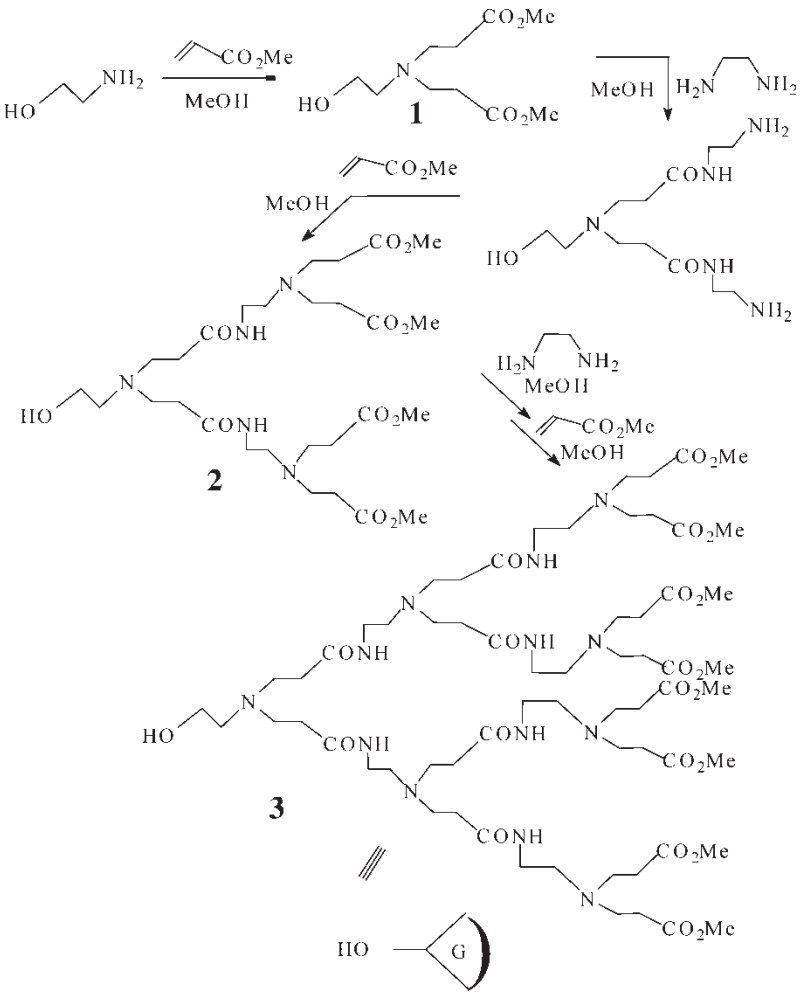

SCHEME 1

dendrimers **4–6** display a broad asymmetric absorption band due to N—H stretching at ~3380 cm^{-1}. Bands occurring in the range 2860–2940 cm^{-1} are associated with symmetric and asymmetric C—H stretching vibrations of the aliphatic —CH_2— and —CH_3 groups. Other spectral features include the ester C═O stretching at 1734 and 1657 cm^{-1} (amide-I, aryl C═C and aryl CH), δ (NH) with ν(CO—N) amide-II at 1550 cm^{-1} and the fingerprint region below 1500 cm^{-1}. Bands at ~1209 and ~1051 cm^{-1} are assigned to the stretching vibration of the ester group (—CO—O—C—).

^{1}H NMR spectra of **4–6** clearly show the presence of the naphthalene core in the dendrimer structures. Thus the peaks in the region 7.75–7.27 ppm were found to be due to the naphthalene ring hydrogens. The ^{1}H NMR spectra also show peaks at 2.76, 1.6 and 1.24 ppm due to the sebacic acid unit. All other peaks due to the dendritic units appear at their

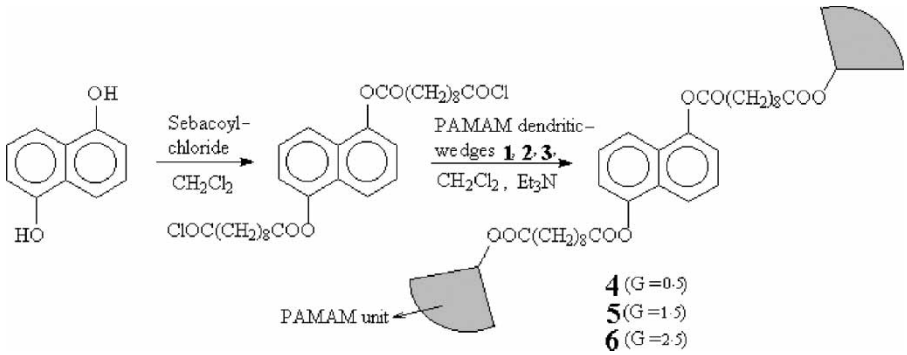

SCHEME 2

usual positions. ^{13}C NMR spectra of both **5** and **6** display the expected carbon signals. Peaks in the region 174–172 ppm are associated with the ester and amide carbonyl carbons. Signals that are assigned to the aromatic carbons of naphthalene unit appear at 146.7, 128.1, 125.9, 119 and 118 ppm, and signals due to sebacic acid carbons appear at 29–24 ppm. Other resonance peaks associated with the methylene and methyl carbons of PAMAM units appear at their usual positions as presented later. The expected CHN percentages obtained from the elemental analysis reaffirms the dendritic structures **5** and **6**.

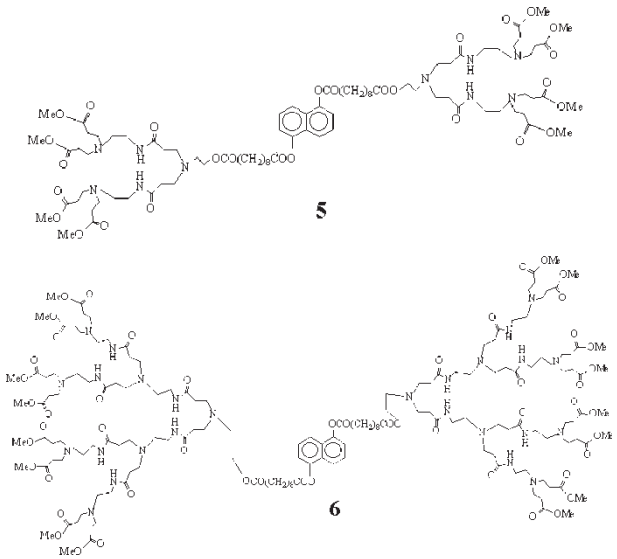

5

6

Fluorescence Properties

Naphthalene systems are fascinating chromophores on account of their interesting and potentially useful luminescence characteristics. We have established the luminescence behavior of the naphthalene-centered dendrimers **5** and **6**. Figures 1 and 2 present the fluorescence spectra of **5** and **6** in $CHCl_3$ and

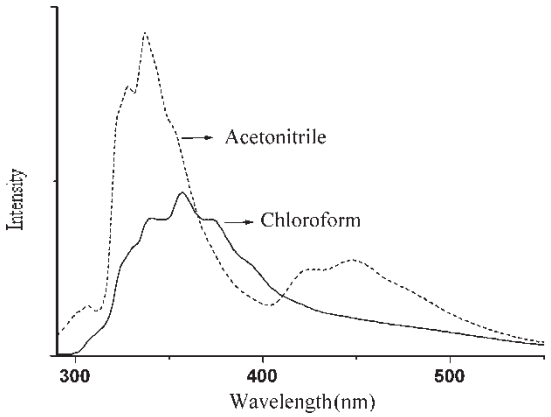

FIGURE 1 Fluorescence spectra of **6** ($\sim 2 \times 10^{-5}$ M) in acetonitrile and chloroform solvents; $\lambda_{exc} = 280$ nm.

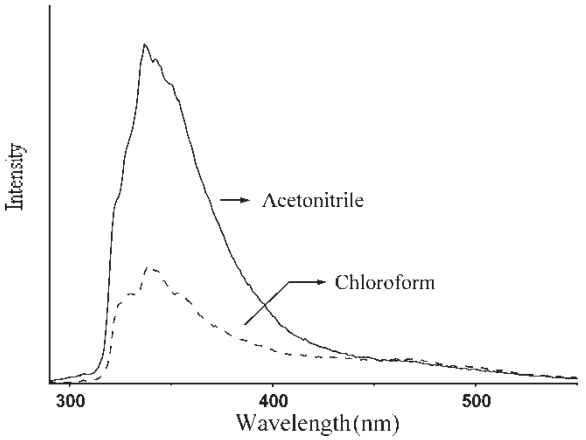

FIGURE 2 Fluorescence spectra of **5** ($\sim 6 \times 10^{-5}$ M) in acetonitrile and chloroform solvents; $\lambda_{exc} = 280$ nm.

acetonitrile. The fluorescence band maxima for **5** and **6** in $CHCl_3$ occur at 336 and 357 nm, respectively, while in acetonitrile solutions, the maxima appear at 336 and 337 nm, respectively, when excited at 280 nm (Table I).

The bathochromic shifts of the fluorescence spectra in chloroform solution suggest that the naphthyl core encounters a more polar micro-environment as the dendrimer generation increases from 1.5 to 2.5. However, this bathochromic shift is less ($\Delta\lambda^{F}_{max} = 2$ nm) in more polar solvents (e.g. acetonitrile) probably due to the decrease in polarity around the fluorophore unit. In addition, no appreciable bathochromic shift with solvent polarity was observed in **5**, probably indicating the lack of dendritic environmental polarity surrounding the naphthyl unit. The molecular modeling of **5** and **6** as shown in Figs. 3 and 4 further predicts that the naphthyl fluorophore unit is more confined within the dendritic interior of **6** compared with **5**.

Furthermore, **5** and **6** exhibit broad band excimer signal [7,17,18] at $\lambda_{max} = 425–450$ nm. The relative intensity of the monomer and excimer emission bands was dependent on solvent polarity, indicating intermolecular excimer formation, as was also shown in our earlier investigation [7]. However, in chloroform solution the probability of excimer formation decreases with an increase in the generation due to the more crowded environment around the fluorophore unit. In acetonitrile solution, however, the excimer emission was observed to be intense in **6** and less pronounced in **5**. This might be

TABLE I Photophysical characteristics of **5** and **6** excited at 280 nm at 27°C

Dendrimer	Solvent	λ_{abs} (nm)	λ_F (nm)
5	$CHCl_3$	270–285	338
	CH_3CN	280	336
6	$CHCl_3$	272–285	357
	CH_3CN	281	338

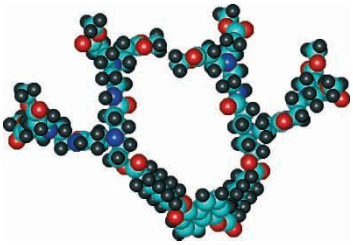

FIGURE 3 Optimized geometry of **5**, $E_{min} = 82.89\,kcal\,mol^{-1}$, C= ●, N= ●, O = ●, H= ●.

related to the change in H-bonded interactions and overall conformation that favor the pronounced excimer formation in **6**.

Change in Fluorescence on Carboxylic Acid Binding

In our recent paper [7] we reported the carboxylic acid-sensitive fluorescence signal amplification of **6**. In this present paper we have investigated the luminescence behavior of **5** and **6** in chloroform upon addition of carboxylic acids, e.g. acetic acid (AcOH) and trifluoroacetic acid (TFA). We found that the fluorescence intensities of both **5** and **6** gradually decreased on successive addition of AcOH and TFA, as shown in Figs. 5–8. The observed quenching of the centrally placed naphthalene emission upon addition of TFA or AcOH is probably associated with intimate interactions of the naphthalene excited state with the amide and ester subunits as well as carboxylate counter anions originating from the protonation of the amine subunits [19]. Interestingly, with addition of the stronger acid TFA, the fluorescence quenching becomes much more efficient, as shown in Figs. 6 and 8, indicating better complexation (e.g. H-bonding) of the amide and ester subunits as well as the protonation of amine groups. Furthermore, the gradual reduction in fluorescence intensities with successive addition of AcOH/TFA implies a progressive increase in the molecular environmental polarity of the fluorophore residue. Moreover, with addition of TFA, the fluorescence quenching became much more efficient, as

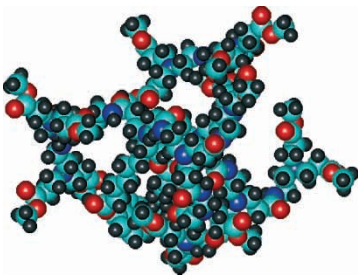

FIGURE 4 Optimized geometry of **6**, $E_{min} = 91.38\,kcal\,mol^{-1}$, C= ●, N= ●, O = ●, H= ●.

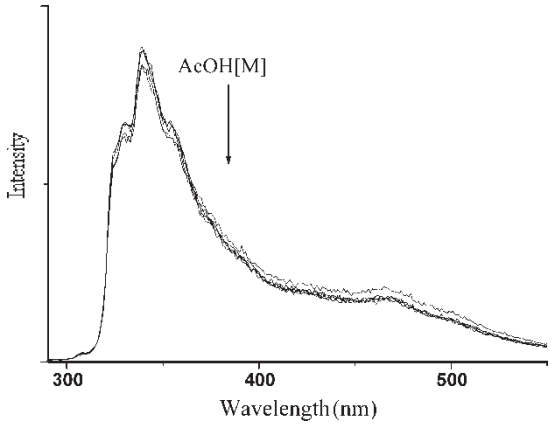

FIGURE 5 Fluorescence spectral changes in **5** ($\sim 6\times10^{-5}$ M) in $CHCl_3$ (27°C, $\lambda_{exc} = 280$ nm) upon addition of AcOH.

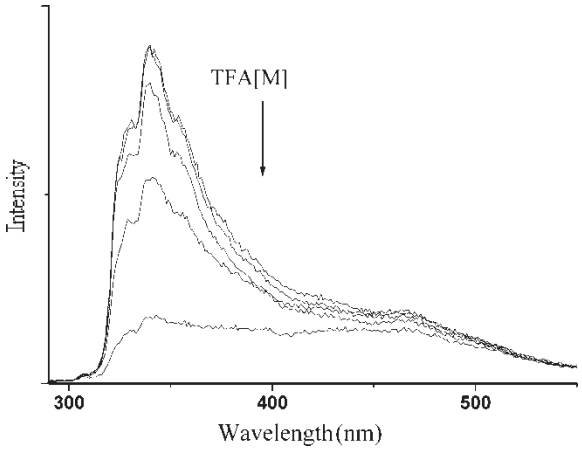

FIGURE 6 Fluorescence spectral changes in **5** ($\sim 6\times10^{-5}$ M) in $CHCl_3$ (27°C, $\lambda_{exc} = 280$ nm) upon addition of TFA.

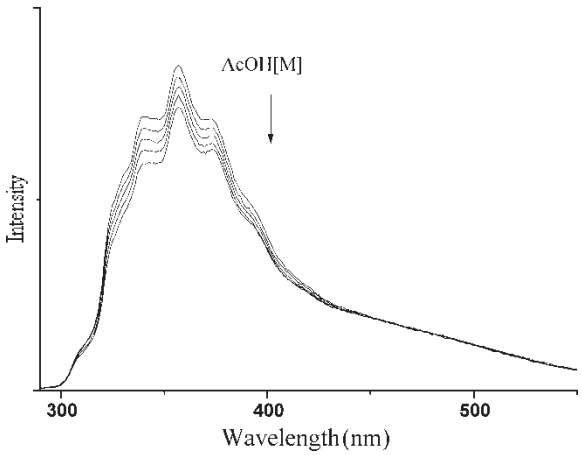

FIGURE 7 Fluorescence spectral changes in **6** ($\sim 2\times10^{-5}$ M) in $CHCl_3$ (27°C, $\lambda_{exc} = 280$ nm) upon addition of AcOH.

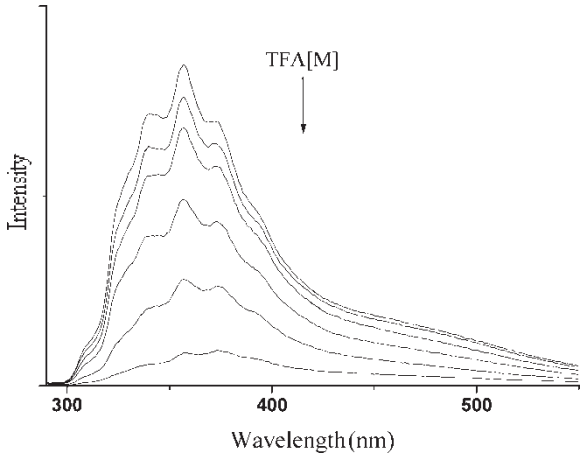

FIGURE 8 Fluorescence spectral changes in **6** ($\sim 2\times10^{-5}$ M) in $CHCl_3$ (27°C, $\lambda_{exc} = 280$ nm) upon addition of TFA.

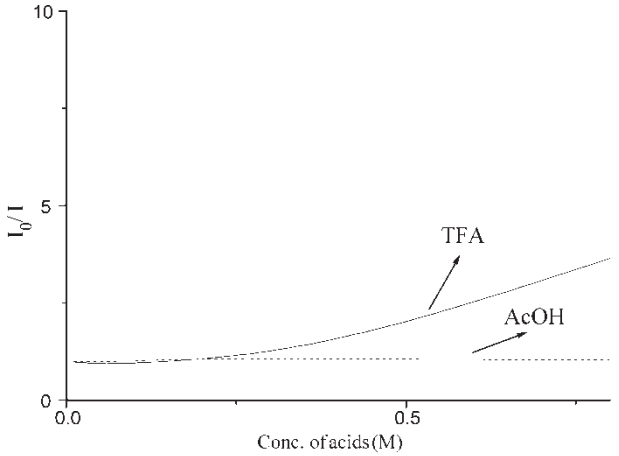

FIGURE 9 Stern–Volmer plot of I_0/I *vs.* concentration of acids for **5**.

shown in Figs. 6 and 8, due to better complexation (e.g. H-bonding) as well as protonation of the amine subunits in **5** and **6**, ascribing the significant enhancement of the local polarity surrounding the naphthyl residue. In this context, the protonation of the amine groups results in increase in polarity probably inducing the main effect on the optical properties. This complexation behavior was further supported by ^{1}H NMR spectroscopy. In agreement with our previous observations [7], addition of TFA to a $CDCl_3$ solution of, for instance, dendrimer **6** caused the facile protonation of the tertiary nitrogens, as evidenced by the appearance of ammonium groups at 7.5 ppm.

Significant broadening of the dendritic $CONHCH_2$ protons at 3.30 ppm and a moderate downfield shift of the methyl ester protons ($\Delta\delta = 0.04$ ppm) were also observed, indicating strong complexation. On the other hand, similar but weak complexaion events were also noted for weaker acid AcOH but no signal due to the ammonium groups was evident in the region 7.5–7.3 ppm, suggesting its inability to quaternize tertiary nitrogens. The Stern–Volmer plots (Figs. 9 and 10) showed stronger quenching with TFA than AcOH demonstrating the better chemosensitivity of **5** and **6** for TFA.

Change in Fluorescence on Metal Binding

Study of fluorescence modulation in dendritic systems in the presence of metal ions [20–23] has also attracted considerable interest because of their branched architectures and the presence of a large number of co-ordinating sites in the interior. Typical change in the fluorescence behavior of **5** and **6** induced by metal ions, e.g. Zn(II) ($\sim10^{-5}$ M, as $Zn(OAc)_2{\cdot}2H_2O$) and Cu(II) ions ($\sim10^{-5}$ M for as $Cu(OAc)_2{\cdot}xH_2O$) is illustrated in Figs. 11–14. Addition of photophysically inactive Zn(II) ions, as $Zn(OAc)_2{\cdot}2H_2O$, to the acetonitrile solution of **5** and **6** leads to a marginal increase in emission intensity (Figs. 11 and 13). However, strong fluorescence quenching in **5** and **6** upon addition of photophysically active Cu(II) ions as $Cu(OAc)_2$ xH_2O, as shown in Figs. 12 and 14, may be attributed to energy transfer quenching between the naphthyl excited state and Cu(II), complexed into the polyamidoamine dendritic skeletons.

EXPERIMENTAL

Materials and Methods

Methylacrylate was shaken with a 5% NaOH solution, washed with water, dried over Na_2SO_4 and distilled. Ethylenediamine was used as received without further purification. FT-IR spectroscopic measurements in KBr pellets were carried out using a Thermo-Nicolate Nexus-870 FT-IR spectrometer. NMR spectra were recorded on a Bruker AC200 spectrometer using $CDCl_3$ as solvent. CHN analyses

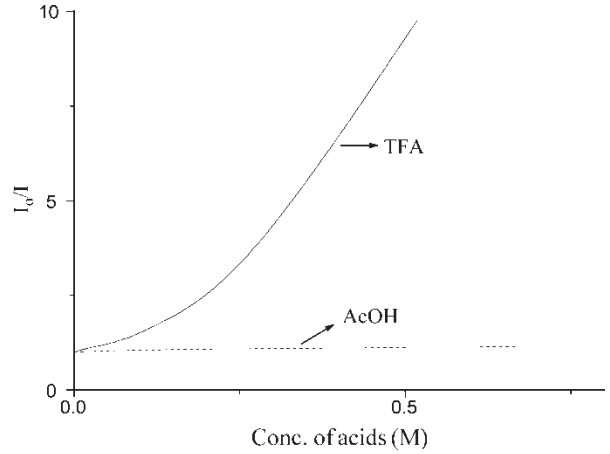

FIGURE 10 Stern–Volmer plot of I_0/I *vs.* concentration of acids for **6**.

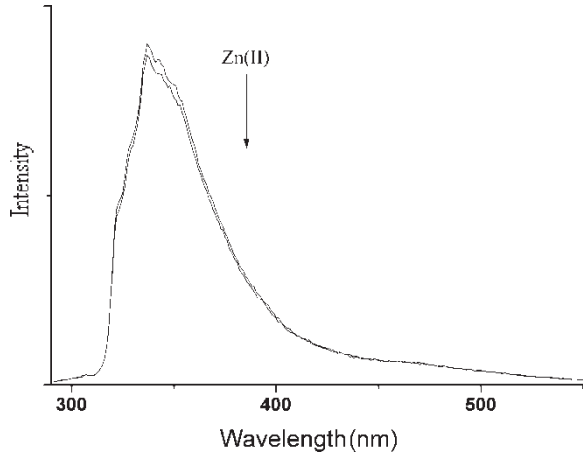

FIGURE 11 Fluorescence spectral changes in **5** upon the addition of Zn(II) ions in acetonitrile ($\lambda_{exc} = 280$ nm) at 27°C.

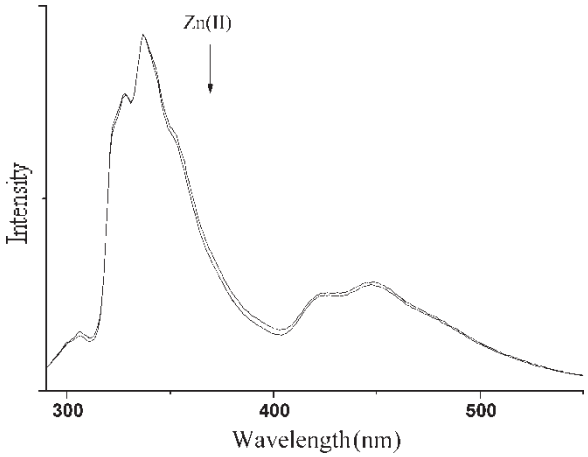

FIGURE 13 Fluorescence spectral changes in **6** upon the addition of Zn^{+2} ions in acetonitrile ($\lambda_{exc} = 280$ nm) at 27°C.

of the dendrimer were obtained using a 2400 Series II CHN analyzer (Perkin-Elmer, USA), using helium as driving gas and oxygen as combustion gas. MALDI-TOF mass spectral measurement of **6** was carried out on a Biospectrometry Voyager-DE PROs instrument using a cinnamic acid matrix. For fluorescence measurements a Shimadzu absorption spectrophotometer (UV-1601) and a Spex-fluorolog-3 spectrofluorimeter (FL3-11) were used. Molecular modeling calculation was carried out using molecular mechanics (MM^+) of Hyper Chem 7.

Synthesis of PAMAM Dendritic Wedges 1–3

Divergent synthesis (Scheme 1) of the ester-terminated PAMAM dendritic wedges was carried out by initial Michael addition of methanolic solution of ethanolamine (2 g, 0.03 mol) with excess methylacrylate (28.2 g, 0.3 mol) (1:10 mol ratio). The reaction mixture was stirred for 3 days at room temperature. Excess methylacrylate was removed under vacuum to afford the ester-functionalized derivative **1**, which was then submitted to the reaction sequences leading to the generation of **2**, consisting of the exhaustive amidation of **1** with ethylenediamine (1:30 mol ratio), followed by Michael addition of the resulting amine with methylacrylate (8 equiv. of **1**). Repetition of this two-step procedure ultimately leads to the next generation **3**. The dendritic wedges **2** and **3**, isolated in 85–90% yield, were gummy in nature.

Selected data for **2**: FT-IR (KBr): cm^{-1}: 3378, 3269 (broad, OH, NH, both free and H-bonded), 2929, 2840 (C—H of CH_3 and CH_2 groups), 1738 (ester C═O), 1649 (amide-I), 1546 (amide-II), 1437, 1207, 1040 (CO—O—C); ^{1}H NMR (200 MHz, $CDCl_3$) δ: 7.14 (bs, 2H, all —CON*H*—), 3.68 (s, 13H, $-CO_2CH_3$, HO—CH_2—), 3.28–3.25 (bm, 4H, —CONH—CH_2—), 2.83–2.70 (bm, 12H, $CONHCH_2$ CH_2N, $NCH_2CH_2CO_2Me$), 2.60–2.35 (m, 19H, all other —CH_2—, *H*O—CH_2—). Elemental analysis for $C_{28}H_{51}N_5O_{11}$(%): C, 53.07; H, 8.11; N, 11.04; found: C, 52.67, H, 7.88; N, 10.7%.

Selected data for dendritic wedge **3**: FT-IR (KBr): cm^{-1}: 3410, 3250 (broad, OH, NH, both free and

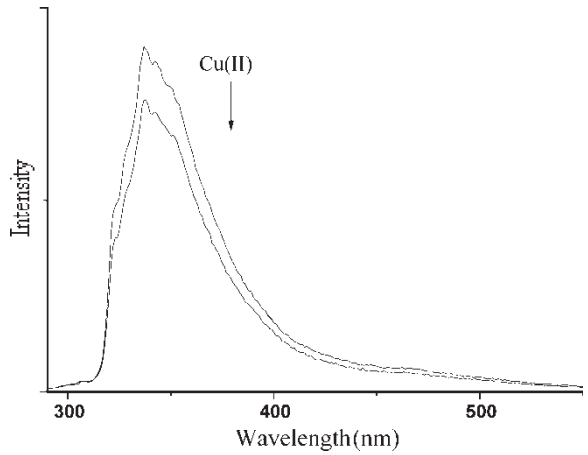

FIGURE 12 Fluorescence spectral changes in **5** upon the addition of Cu(II) ions in acetonitrile ($\lambda_{exc} = 280$ nm) at 27°C.

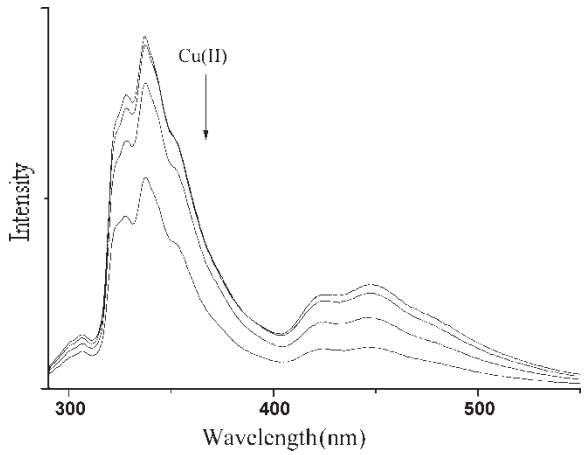

FIGURE 14 Fluorescence spectral changes in **6** upon the addition of Cu(II) ions in acetonitrile ($\lambda_{exc} = 280$ nm) at 27°C.

H-bonded), 2955, 2846 (C—H of CH_3 and CH_2 groups), 1738 (ester C═O), 1655 (amide-I), 1591 (amide-II), 1437, 1373, 1207, 1040 (CO—O—C); ^{1}H NMR (200 MHz, $CDCl_3$) δ: 3.66 (s, 26H, —CO_2CH_3, HO—CH_2—), 3.29–3.27 (m, 12H, —CONH—CH_2—), 2.84–2.70 (bm, 28H, $CONHCH_2CH_2N$, NCH_2CH_2 CO_2Me), 2.58–2.37 (m, 43H, all other —CH_2—, $HOCH_2$—). ^{13}C NMR (50 MHz, $CDCl_3$) δ: 177.1 (NC═O; out), 174.1 (NC═O, in), 172.3 (C═O), 56.8, 56.1, 52.2, 51.2, 50.2, 49.9, 49.2, 45.1, 42.4, 37.7, 36.9, 32.5, 32. MALDI-TOF MS: m/z calcd for $C_{64}H_{115}N_{13}O_{23}$: 1472.6 $[M + K]^+$; found: 1473.0 $[M + K]^+$. Elemental analysis calcd (%): C, 53.58; H, 8.08; N, 12.69; found: C, 53.31, H, 7.83; N, 12.43%.

Synthesis of Naphthalene-based PAMAM Dendrimers 4–6

1,5-Dihydroxynathphalene was added portionwise to a stirred solution of sebacoyl chloride in dry CH_2Cl_2. The mixture was warmed and stirred for 1 h and then PAMAM dendritic wedge (2 equivalents of naphthalene-embedded sebacoyl chloride) in dry CH_2Cl_2 containing triethylamine was added to the reaction mixture. After stirring overnight, the mixture was quenched with water (20 mL). The organic layer was separated, washed with aqueous $NaHCO_3$ solution and dried over anhydrous Na_2SO_4, filtered and concentrated to afford gummy-like product. Purification was done by column chromatography using $CHCl_3$:MeOH (5:1) as element to obtain the dendrimer in 50–55% yield.

Dendrimer 4

>FT-IR (KBr) cm^{-1}: 3440 (—NH str.), 2920, 2850 (—CH_2—, —CH_3 str.), 1734 (ester C═O str.), 1261 (CO—O—C str.), 1021 (CO—O—C str.), 800. ^{1}H NMR (200 MHz, $CDCl_3$) δ (ppm) = 7.76 (d, J = 8 Hz, 2H), 7.52 (m, 2H), 7.40 (s, 2H), 3.67 (bs, 16H, —CO_2CH_3, —$COOCH_2CH_2N$—), 2.91–2.73 (bm, 12H, —$(CH_2)_8$—$CO_2CH_2CH_2N$—CH_2CH_2—), 2.53–2.46 (bm, 8H, —$NCH_2CH_2CO_2CH_3$), 2.37–2.26 (bm, 8H, all other dendritic CH_2, —$OCOCH_2(CH_2)_6CH_2COO$— of sebacic acid), 1.62 (bm, 8H, naph-$OCOCH_2CH_2(CH_2)_4CH_2CH_2COO$—), 1.24–1.30 (bm,16H,naph-$OCO(CH_2)_2(CH_2)_4$—). Elemental analysis calcd for $C_{50}H_{74}N_2O_{16}$: C, 62.62; H, 7.77; N, 2.92; found: C, 62.48; H, 7.62; N, 2.81.

Dendrimer 5

FT-IR (KBr) cm^{-1}: 3446 (—NH str.), 2929, 2853 (—CH_2—, —CH_3 str.), 1734 (ester C═O str.), 1647 (amide-I, aryl C═C, aryl CH str.), 1541 (amide-II str.), 1436, 1362, 1201 (CO—O—C str.), 1044 (CO—O—C str.), 800. ^{1}H NMR (200 MHz, $CDCl_3$) δ (ppm) = 7.75 (d, J = 8 Hz, 2H), 7.45 (t, J = 8 Hz, 2H), 7.27(d, J = 6 Hz, 2H), 3.68 (s, 28H, —CO_2CH_3, —$COOCH_2CH_2N$—), 3.30 (bm, 8H, —$CONHCH_2$—), 2.79–2.61 (bm, 36H, —$(CH_2)_8$—$CO_2CH_2CH_2N$—CH_2 CH_2—, —$NCH_2CH_2CO_2CH_3$, —$CONHCH_2CH_2N$—), 2.52–2.30 (bm, 24H, all other dendritic CH_2, —$OCOCH_2(CH_2)_6CH_2COO$— of sebacic acid), 1.6 (bm, 8H, naph-$OCOCH_2CH_2(CH_2)_4CH_2CH_2COO$—), 1.24–1.29 (bm, 16H, naph-OCO—$(CH_2)_2$ —$(CH_2)_4$—). ^{13}C NMR (50 MHz, $CDCl_3$) δ (ppm) 173.4, 172.0 (CONH, —$COOCH_3$, —$COOCH_2$—, naph-$OCOCH_2$), 146.7, 128.2, 125.9, 119.0, 118.7, 52.9, 51.6, 51.4, 50.7, 49.9, 49.2, 37.1, 34.3, 29.0, 24.9, 24.8. Elemental analysis calcd for $C_{86}H_{138}N_{10}O_{28}$(%): C, 58.69; H, 7.90; N, 7.96; found: C, 58.44; H, 7.67; N, 7.82.

Dendrimer 6

FT-IR (KBr) cm^{-1}: 3346 (—NH str.), 2925, 2853 (—CH_2—, —CH_3 str.), 1733 (ester C═O str.), 1652 (amide-I, aryl C═C, aryl CH str.), 1541 (amide-II str.), 1435, 1384, 1201 (CO—O—C str.), 1033 (CO—O—C str.), 799. ^{1}H NMR (200 MHz, $CDCl_3$) δ (ppm) 7.75 (d, J = 8 Hz, 2H), 7.45 (m, 2H), 7.27(s, 2H), 3.66 (bs, 52H, —CO_2CH_3, —$COOCH_2CH_2N$—), 3.29 (bs, 24H, —$CONHCH_2$—), 2.29–2.74 (bm, all other dendritic CH_2, —$OCOCH_2(CH_2)_6CH_2COO$— of sebacic acid, 148H), 1.6 (bm, 8H, naph-$OCOCH_2$ $CH_2(CH_2)_4CH_2CH_2COO$—),1.24–1.29 (bm, 16H, naph$OCO(CH_2)_2(CH_2)_4$—). ^{13}C NMR (50 MHz, $CDCl_3$) δ (ppm) = 173, 172 (CONH, —$COOCH_3$, —$COOCH_2$—, naph—$OCOCH_2$), 146.6, 128.1, 125.9, 119, 118, 52.8, 51.6, 51.3, 50.2–49.2 (broad and unresolved), 37, 34.3, 34, 33–32.6 (unresolved), 29, 24.9, 24.8. MALDI-TOF MS: m/z calcd for $C_{158}H_{266}N_{26}O_{52}$ 3362.44 $[M + H]^+$; found: 3367.72 $[M + H]^+$; Elemental analysis calcd (%): C, 56.45; H, 7.97; N, 10.83; found: C, 56.28; H, 7.79; N, 10.55.

CONCLUSION

We have thus synthesized naphthalene fluorophore-based PAMAM dendrimers (G = 0.5–2.5) and investigated the influence of the solvent polarity on their photophysical characteristics. These novel dendrimers were found to exhibit a higher level of fluorescence quenching towards TFA in comparison to AcOH. Their fluorescence behavior was also been studied in the presence of metal salts $Zn(OAc)_2{\cdot}xH_2O$ and $Cu(OAc)_2{\cdot}xH_2O$, and they exhibit significant fluorescence quenching towards Cu(II) ions. The anticipated transduction of recognition events based on the complexation of guest molecules, for instance carboxylic acids and metal ions at a high density, with dendritic functional subunits into a fluorescence signal, positioning other fluorophore units at the core of these PAMAM dendritic systems represents a fascinating challenge.

Further studies in our laboratory are in progress to explore the synthesis of more elaborate fluorophore-labeled PAMAM dendritic systems and their fluorescence chemosensing events.

References

[1] de Silva, A. P.; Gunaratne, H. Q. N.; Gunnlaugsson, T.; Huxley, A. J. M.; McCoy, C. P.; Rademacher, J. T.; Rice, T. E. *Chem. Rev.* **1997**, 1515.

[2] Sakamoto, M.; Ueno, A.; Mihara, H. *J. Chem. Soc., Chem. Commun.* **2000**, *1741*, and references therein.

[3] Gilat, S. L.; Adronov, A.; Frechet, J. M. J. *J. Org. Chem.* **1999**, *64*, 7474.

[4] Balzani, V.; Ceroni, P.; Gestermann, S.; Kauffmann, C.; Gorka, M.; Vogtle, F. *J. Chem. Soc., Chem. Commun.* **2000**, 853.

[5] Cardona, C. M.; Alvarez, J.; Kaifer, A. E.; McCarley, T. D.; Pandey, S.; Baker, G. A.; Bonzagni, N. J.; Bright, F. V. *J. Am. Chem. Soc.* **2000**, *122*, 6139, and references therein.

[6] Balzani, V.; Ceroni, P.; Gestermann, S.; Gorka, M.; Kauffmann, C.; Vogtle, F. *Tetrahedron* **2002**, *58*, 629.

[7] Ghosh, S.; Banthia, A. K. *Tetrahedron Lett.* **2002**, *43*, 6459.

[8] Grabchev, I.; Bojinov, V.; Chovelon, J. M. *Polymer* **2003**, *44*, 4421.

[9] Grabchev, I.; Chovelon, J. M.; Bojinov, V.; Ivanova, G. *Tetrahedron* **2003**, *59*, 9591, and references therein.

[10] Bosman, A. W.; Janssen, H. M.; Meijer, E. W. *Chem. Rev.* **1999**, *99*, 1665.

[11] Tomalia, D. A.; Naylor, A. M.; Goddard, W. A. *Angew. Chem., Int. Ed. Engl.* **1990**, *29*, 138.

[12] Pistolis, G.; Malliaris Tsiouravas, D.; Paleos, C. *Chem. Eur. J.* **1999**, *5*, 1440.

[13] Ghosh, S.; Banthia, A. K. *Tetrahedron Lett.* **2001**, *42*, 501.

[14] Ghosh, S.; Banthia, A. K. *J. Polym. Sci., Part A, Polym. Chem.* **2001**, *39*, 4182.

[15] Ghosh, S.; Banthia, A. K.; Maiya, B. G. *Organic Lett.* **2002**, *4*, 3603, and references therein.

[16] Takaguchi, Y.; Sako, Y.; Yanagimoto, Y.; Tsuboi, S.; Motoyoshiya, J.; Aoyama, H.; Wakahara, T.; Akasaka, T. *Tetrahedron Lett.* **2003**, *44*, 5777.

[17] Parker, D.; Williams, J. A. G. *J. Chem. Soc., Perkin Trans. 2* **1995**, 1305.

[18] Albelda, M. T.; Bernardo, A. M.; Diaz, P.; Espana, E. G.; Melo, J. S.; Pina, F.; Soriano, C.; Luis, S. V. *J. Chem. Soc., Chem. Commun.* **2001**, 1520.

[19] Caminati, G.; Turro, N. J.; Tomalia, D. A. *J. Am. Chem. Soc.* **1990**, *112*, 8515.

[20] Vogtle, F.; Gestermann, S.; Kauffmann, C.; Ceroni, P.; Vicinelli, V.; Balzani, V. *J. Am. Chem. Soc.* **2000**, *122*, 10398.

[21] Grabchev, I.; Qian, X.; Bojinov, V.; Xiao, Y.; Zhang, W. *Polymer* **2002**, *43*, 5731.

[22] Kim, Y. H. *J. Polym. Sci., Part A, Polym. Chem.* **1998**, *36*, 1685, and references therein.

[23] Voit, B. *J. Polym. Sci., Part A, Polym. Chem.* **2000**, *38*, 2505.